

PAPER • OPEN ACCESS

## Numerical investigations of bistable piezoelectric cantilever for enhanced energy harvesting

To cite this article: M A Abdelnaby *et al* 2020 *IOP Conf. Ser.: Mater. Sci. Eng.* **973** 012022

View the [article online](#) for updates and enhancements.

You may also like

- [Analysis of broadband characteristics of two degree of freedom bistable piezoelectric energy harvester](#)  
Dan Zhao, Minyao Gan, Chihang Zhang et al.
- [Multi-frequency array of nonlinear piezoelectric converters for vibration energy harvesting](#)  
Marco Baù, Davide Alghisi, Simone Dalola et al.
- [A review on energy harvesting approaches for renewable energies from ambient vibrations and acoustic waves using piezoelectricity](#)  
Riaz Ahmed, Fariha Mir and Sourav Banerjee



The Electrochemical Society  
Advancing solid state & electrochemical science & technology

243rd Meeting with SOFC-XVIII

Boston, MA • May 28 – June 2, 2023

Accelerate scientific discovery!

Learn More & Register



# Numerical investigations of bistable piezoelectric cantilever for enhanced energy harvesting

M A Abdelnaby<sup>1</sup>, M S Shiba<sup>2</sup> and S Ali<sup>3</sup>

<sup>1</sup>Production Engineering and Printing Technology Department, Akhbar El Yom Academy, Egypt

<sup>2</sup>Automotive Engineering Department, Higher Technology Institute, 10<sup>th</sup> of Ramadan 6<sup>th</sup> of October, Egypt

<sup>3</sup>Department of Mechatronics, Canadian International College, Cairo, Egypt  
E-mail: [muhmmad.aly@akhbaracademy.edu.eg](mailto:muhmmad.aly@akhbaracademy.edu.eg)

**Abstract.** Piezoelectric energy harvesting applications have been highly impacted research area recently. Numerical investigations for bistable piezoelectric cantilevers have great importance to understand its dynamic performance. This paper aims to develop comprehensive numerical models to simulate the dynamic response of a unimorph piezoelectric bender under bistability effect for enhanced energy harvesting. To this end, the equivalent stiffness, damping, electromagnetic coupling and capacitance coefficients of a bistable piezoelectric cantilever have been numerically developed. Besides, finite element models are developed to determine the bistability repulsion force between magnets. The resulting simulations are then implemented in an electromechanical model to predict the output voltage and power over a range of load resistance.

## 1. Introduction

Over the last decade, vibration-based energy harvesting has been discussed as a promising field to convert ambient waste energy into useful electrical energy [1-5]. Furthermore, the vibration energy harvesting approach has been developed to power wireless sensor nodes in the structural health monitoring field [6-10]. One of the most promising solutions in this context is using the magnetic bistability piezoelectric systems, which transition from one stable state to another and accordingly enhance the output power over a wider frequency range [11-15]. Some of the developments on bistability piezoelectric energy harvesting have been presented in [16-23].

Previous researches about using piezoelectric cantilever in energy harvesting applications indicate two main theoretical challenges. First, estimating the magnetic repulsion force between a couple of magnets, which often experimentally developed by mounting one magnet on an electronic scale while placing another magnet on an arm that is linearly guided on a movable frame whose displacement is measured by a Vernier caliper [20], [23], after that can be expanding the vector of repulsion force as a function of horizontal gap and vertical elevation difference between magnets. Second, theoretical relations for understanding electromechanical performance of piezoelectric beam are very complicated, especially for multi-layer piezoelectric beams as in [24], [25], so in this paper, the magnetic repulsion force model has been developed to simulate the behavior of repelling magnets at different horizontal gaps and vertical elevations. Also benefited from previous research and linked it in a distinct way have been done to create theoretical relations, which used for estimating equivalent



stiffness and electromechanical coupling coefficients for unimorph piezoelectric beams at different design parameters. All numerical models have been examined by comparing its results with actual parameters of commercial products to ensure the power of this comprehensive study.

The remainder of this paper is structured into five sections. Section 2 presents the design and electromechanical model of the proposed energy harvester. Section 3 presents the comparative numerical analysis of the proposed design and Section 4 presents an electromechanical response for the proposed harvester. Finally, Section 5 is dedicated to conclusions.

## 2. Harvester design and electromechanical model

Figure 1 shows a schematic illustration of the proposed bistable piezoelectric energy harvester. The harvester consists of unimorph piezoelectric cantilever with tip magnet, which repels against another one in front of it. Whole system subjected to vertical sinusoidal excitation as shown in figure 1. The effects of base excitation and repulsion force between magnets, causes a strain in the piezoelectric layer, which generates output voltage across a load resistance.

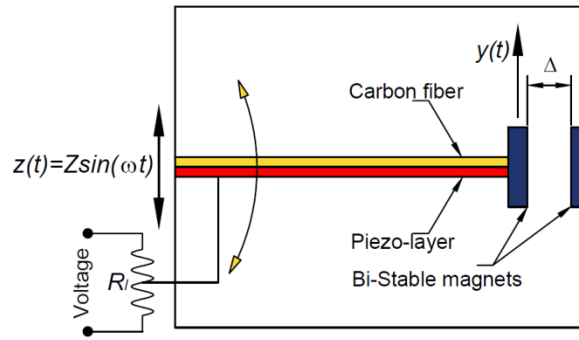


**Figure 1.** Schematic illustration of the proposed harvester.

Electromechanical governing equations for the unimorph piezoelectric cantilever subjected to a repulsion magnetic force as in [23].

$$\begin{bmatrix} m & 0 \\ 0 & 0 \end{bmatrix} \begin{Bmatrix} \ddot{y} \\ \ddot{v} \end{Bmatrix} + \begin{bmatrix} c & 0 \\ \theta & c_p \end{bmatrix} \begin{Bmatrix} \dot{y} \\ \dot{v} \end{Bmatrix} + \begin{bmatrix} k & -\theta \\ 0 & 1/R_l \end{bmatrix} \begin{Bmatrix} y \\ v \end{Bmatrix} = \begin{Bmatrix} F_m \\ 0 \end{Bmatrix} \quad (1)$$

Where:  $m$  [kg],  $k$  [N/m], and  $c$  [Ns/m] are the equivalent mass for piezoelectric cantilever with tip magnet, equivalent stiffness, and equivalent damping, respectively, also  $\theta$  [N/V] is the equivalent electromechanical coupling,  $c_p$  [F] is the equivalent capacitance of piezo layer,  $R_l$  [ $\Omega$ ] is the load resistance,  $y$  [mm] tip displacement,  $v$  [V] is the output voltage and  $F_m$  [N] magnetic repulsion force. In order to solve numerically the electromechanical equations of the model in figure 1 state-space representation will be as follows [23]:

state variables,  $u_1 = y$ ,  $u_2 = \dot{y} = \dot{u}_1$  and  $u_3 = v$ , so equation (1) can write in the form:

$$\begin{aligned} \dot{u}_1 &= u_2 \\ \dot{u}_2 &= -\frac{c}{m}u_2 - \frac{k}{m}u_1 + \frac{\theta}{m}u_3 + \frac{1}{m}F_m \\ \dot{u}_3 &= -\frac{1}{c_p R_l}u_3 - \frac{\theta}{c_p}u_2 \end{aligned} \quad (2)$$

In 2004, the relationship between displacement and charge or force and voltage of the unimorph piezoelectric cantilever beam has been investigated by Park and Moon [24], as follows:

$$\begin{bmatrix} y \\ q \end{bmatrix} = \begin{bmatrix} b_{11} & b_{12} \\ b_{21} & b_{22} \end{bmatrix} \begin{bmatrix} F_m \\ v \end{bmatrix} \quad (3)$$

Where,  $q$ [C] is the charge,  $b_{11}$ [m/N] is a coefficient relating between tip displacement and force,  $b_{12}=b_{21}$ [m/V] are the coefficients relating stiffness and electromechanical coupling and  $b_{22}$  [F] equals to the equivalent capacitance ( $c_p$ ). Detailed equations for  $b_{11}$ ,  $b_{12}=b_{21}$  and  $b_{22}$  were found in [24]. By comparing equations (1 and 3) we can determine equivalent stiffness, capacitance and electromechanical coupling for the unimorph piezoelectric cantilever beam as following:

$$b_{11} = 1/k, \quad b_{12} = b_{21} = \frac{\theta}{k} \text{ and } b_{22} = c_p \quad (4)$$

### 3. Comparative analysis

In order to achieve the main contribution of this study, which is developing a comprehensive numerical analysis to examine the electromechanical behavior of the proposed harvester in figure 1, a commercial piezoelectric cantilever (American Piezo Stripe Actuator 40-2010[26]) and nickel-plated NdFeB of Grade 42, F200-10 (first4magnets[27]) have been selected in this work. Accordingly, the analysis will successively show in four steps.

#### 3.1. Determination of electromechanical parameters

Table 1, demonstrate all required parameters for the selected piezoelectric cantilever, to determine coefficients  $b_{11}$ ,  $b_{12}=b_{21}$  and  $b_{22}$  in equation (3) which used after that to calculate equivalent stiffness, capacitance and electromechanical coupling from equation (4).

**Table 1.** American piezostripe actuator 40-2010 parameters.

Parameters	Values
Piezoelectric constant	$-320 \times 10^{-12}$
Total beam length	60 mm
Piezoelectric layer length	60 mm
Length ratio (piezo layer/total beam)	1
Compliance ratio (piezo layer/carbon fiber)	4
Thickness ratio (carbon fiber/ piezo layer)	0.67
Carbon fiber layer thickness	0.16 mm
Piezoelectric layer thickness	0.24 mm
Cantilever beam width	20 mm
Dielectric constant	3800-1700
Electromechanical coupling factor	$1.7 \times 10^{-12}$

According to previous conditions in this work, the calculated electromechanical parameters for equation (4) will be as follows:

$$b_{11} = 0.0030375 \text{ m/N}, \quad k = 329 \text{ N/m}, \quad b_{12} = -8.8437 \times 10^{-6} \text{ [m/V]}, \quad \theta = -2.9 \times 10^{-3} \text{ [N/V]}, \quad \text{and } b_{22} = c_p = 19,000 \text{ pF.} \quad (5)$$

#### 3.2. Electrostatic model

At this point, the electrostatic module of a finite element package (COMSOL Multi-physics) has been used to analyze and examine the electromechanical parameters, which calculated in section 3.1. By using this model, we can estimate the tip displacement of the piezoelectric beam at certain electric potential volt input.

Figure 2a shows the  $y$ -displacement along a piezoelectric beam with subjected to 100 V (electric potential volt), while figure 2b shows the electric potential across the piezoelectric layer (0-100 V) and figure 2c shows the stresses distribution along the piezoelectric beam. By comparing the value of  $y$ -displacement from the electrostatic model with its calculated value from equations (3-5) finding at 100 V (electric potential), tip displacement is 0.92 mm (electrostatic model) and 0.8844 mm (results from equations (3-5)), which are very close to each other.

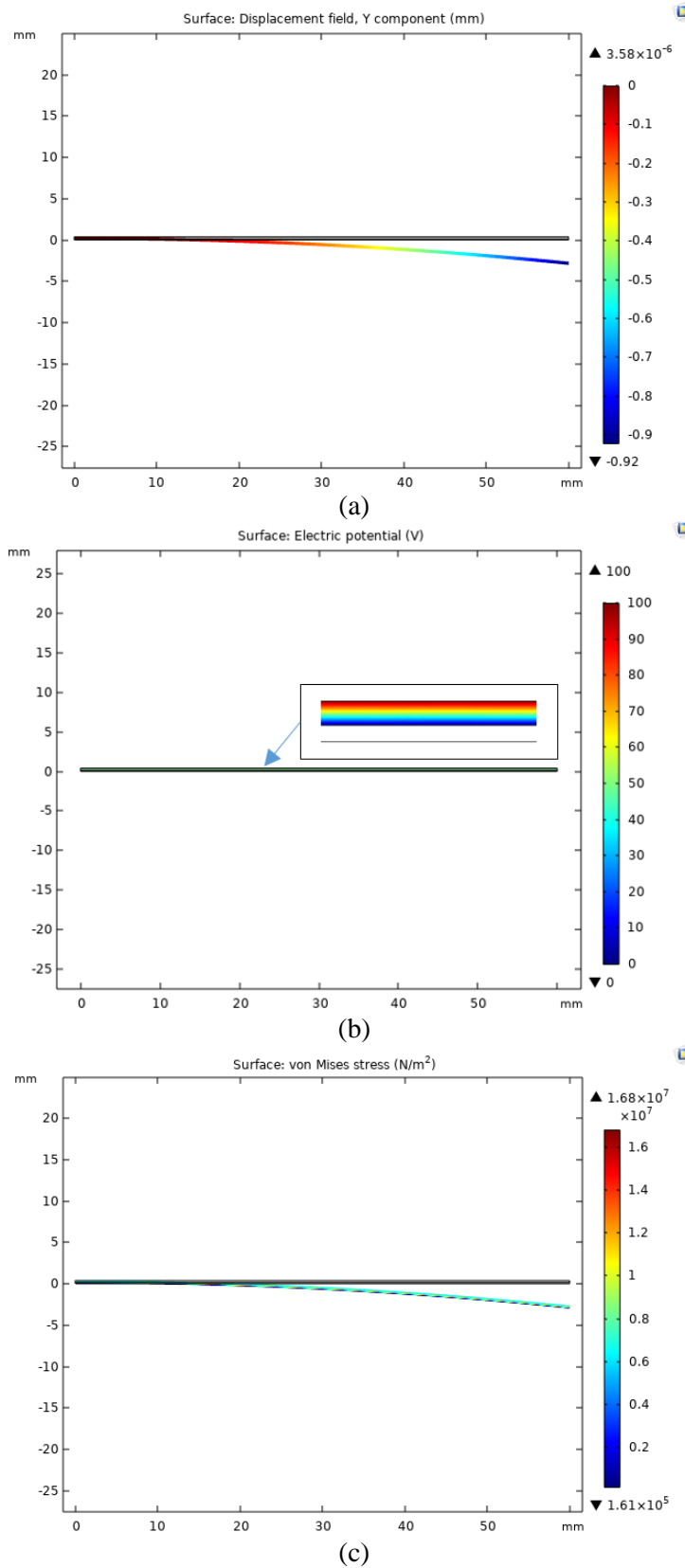


**Figure 2.** Electrostatic finite element model.

### 3.3. Magnetic repulsion force determination

In this section, we discuss the simulation of magnetic repulsion force between two magnets at a defined gap,  $\Delta$  remnant flux density, and vertical elevation difference. Therefore, a finite element model has been developed by using COMSOL Multi-physics to numerically determine the magnetic repulsion force, for a couple of commercial magnets [27] at a gap,  $\Delta = 0.0001$  mm from -40 to 40 mm vertical elevation difference.

Figure 3 shows the two magnets at  $\Delta = 0.0001$  mm, with a refining mesh design that can be achieved by a small fillet radius at magnets corner. Figure 3b and figure 3c shows the magnetic flux density distribution and close view in figure 3d to see the maximum magnetic flux density zone. The physical study in this model has been a magnetic field (no current). The characteristics of the magnet (material, magnetic flux conservation, and magnetic scalar potential) have been imported to the model from the magnets datasheet.

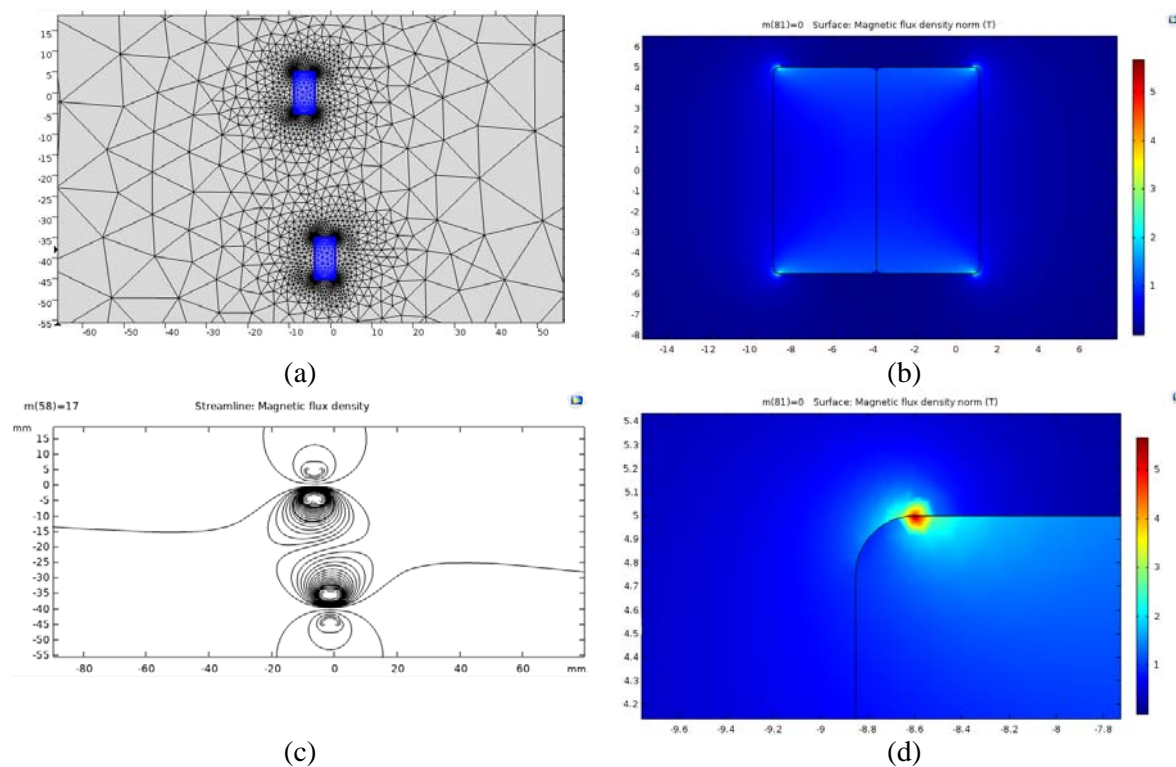


**Figure 3.** Magnetic repulsion force model.

A parametric sweep analysis has been attached to the magnetic field physical study, in order to estimate horizontal and vertical repulsion force between the magnets at different elevation differences, from -40 to 40 mm with step size equals to 1 mm.

Figure 4 shows the magnetic repulsion force in  $X$  and  $Y$  directions with relative vertical distance between the two magnets. It is clear from figure 4 and table 2, that the numerical results compared favorably with the commercial datasheet of the selected magnets.

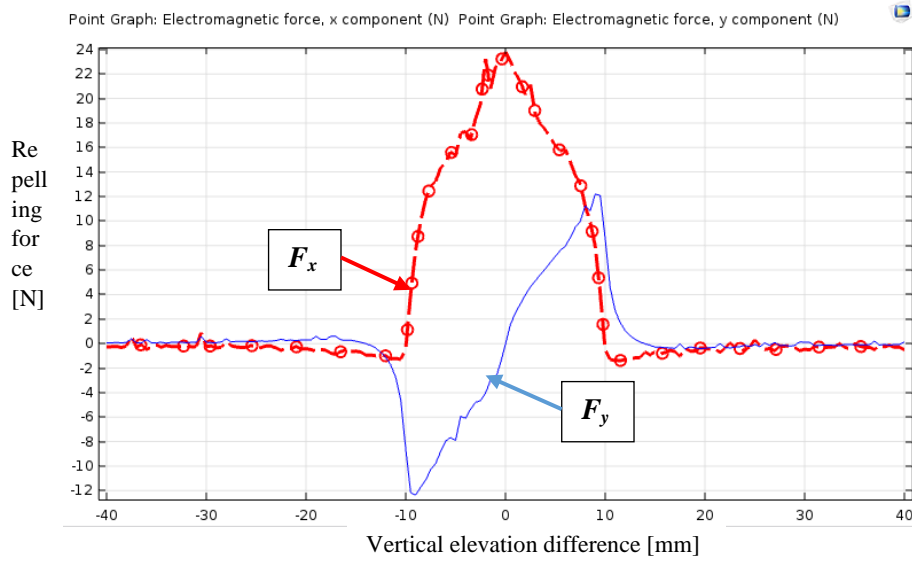


**Figure 4.**Repulsion force versus elevation difference.

**Table 2.**Repulsion force comparisons.




Repulsion force	Data Sheet (KJ-N42)	Finite Element Model	Error %
X direction [N]	22	24 at zero relative distance	≈8
Y direction [N]	11	12.1 at 9.5 mm relative distance	≈9

*3.4. Mechanical characteristics of the piezo beam*

In order to calculate natural frequencies and equivalent damping coefficient of the piezoelectric beam with tip magnet (= 5 g), the numerical models by COMSOL multi-physics have been developed, namely Eigen-frequency and base excitation analysis. Pre-described displacement with 2 mm amplitude and 27 Hz ( $\approx \omega_{n1}$ ) frequency, subjected to the beam root, then measure tip displacements as shown in figure 5 and from the dynamic relations in the case of a base exciting beam, can estimating the equivalent damping coefficient which equals 0.025 N.s/m.

Table 3, shows the first three mode shapes of the piezoelectric cantilever with the tip magnet.

**Table 3.**Eigen-frequency analysis.

First mode shape	Second mode shape	Third mode shape
		
$\omega_{n1} = 28 \text{ Hz}$	$\omega_{n2} = 381 \text{ Hz}$	$\omega_{n3} = 1220 \text{ Hz}$

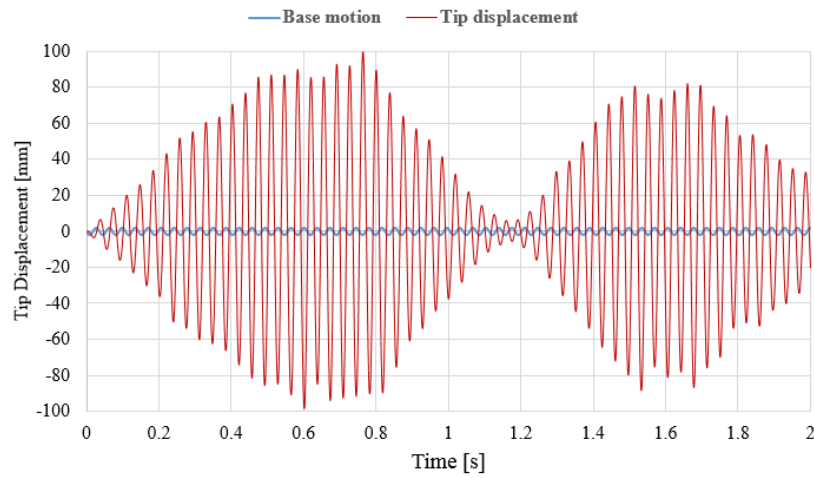


**Figure 5.** Tip displacement response (beating phenomenon).

As a sample figure 6a and figure 6b show the displacement field in Y-direction along the piezoelectric beam at time = 0.82 and 1.046 s, respectively.

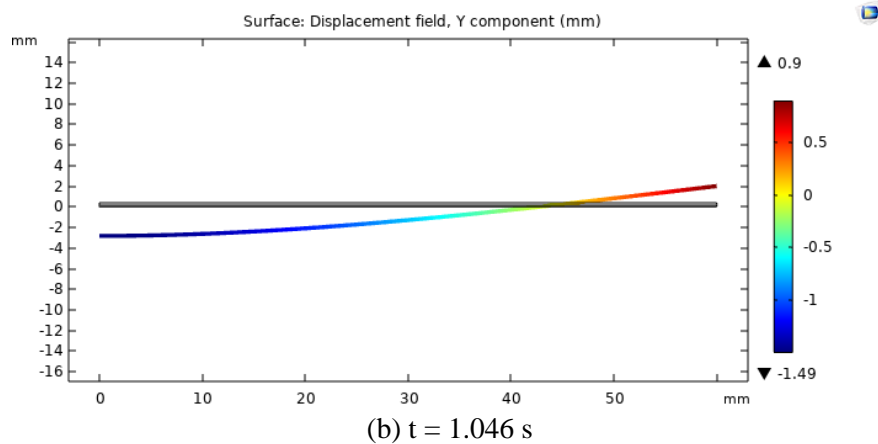
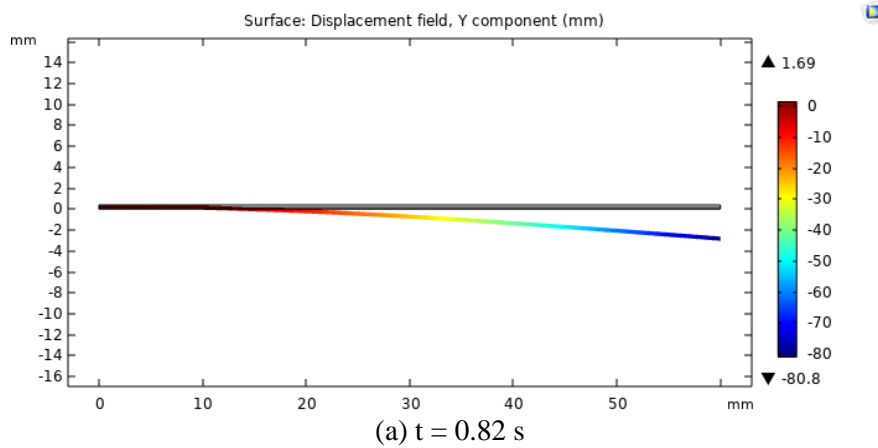


**Figure 6.** Displacement field distribution (base excited beam analysis).



#### 4. Electromechanical response

Afterward, all required parameters to solve equation (1) have been numerically developed and examined by using commercial products. So, the governing ordinary differential equations were numerically solved (*ode15s* command on MATLAB is used in this study) at different load resistances. Figure 7 and figure 8 show the displacement and velocity responses, respectively, at 8 Hz excitation frequency (for low frequency applications), excitation amplitude equals 5 mm, load resistance = 100 k $\Omega$  and gap ( $\Delta = 20$  mm).

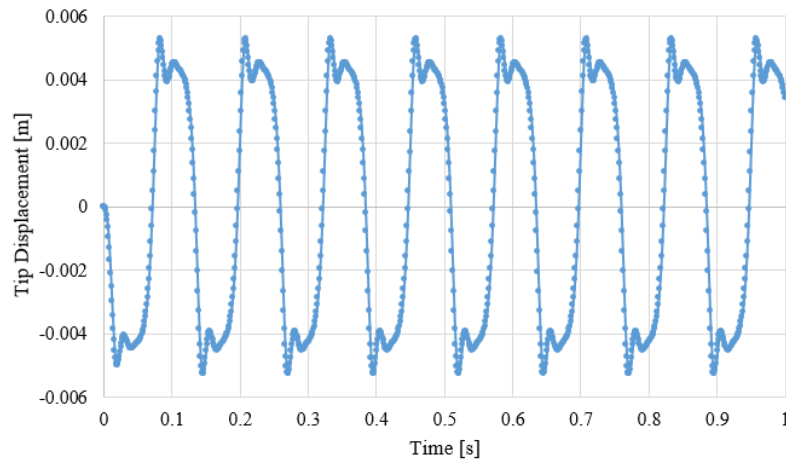


**Figure 7.** Displacement time history.

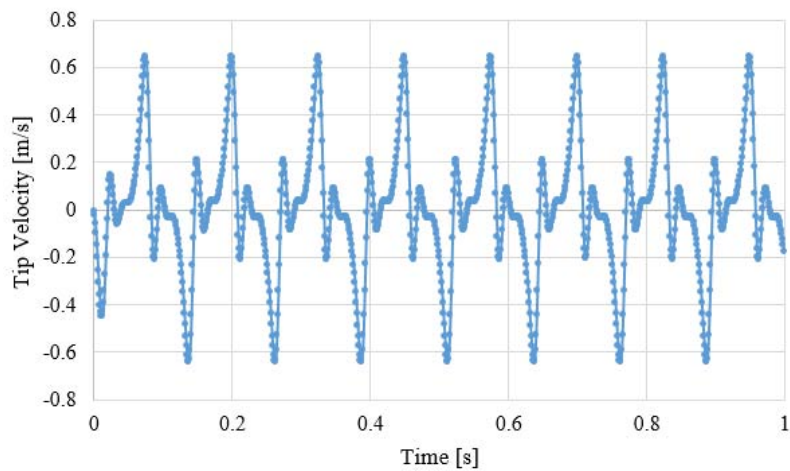


**Figure 8.** Velocity time history.

Figure 9 and figure 10 shows a sample of the time history plot for the output voltage and the output voltage versus load resistance, respectively, at the same conditions for figure 7 and figure 8.

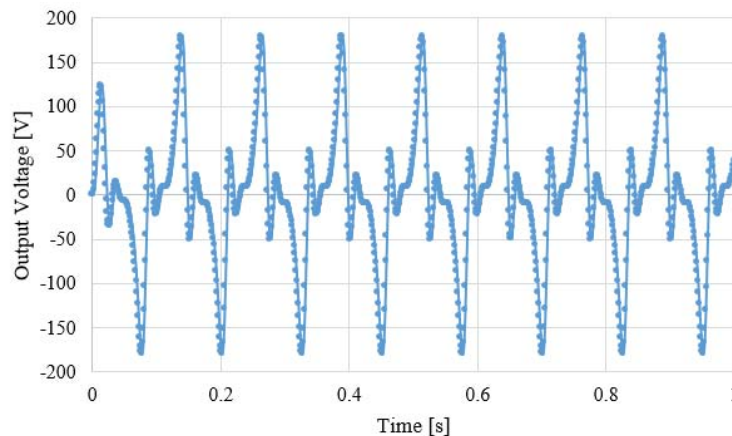


**Figure 9.**Output voltage time history.

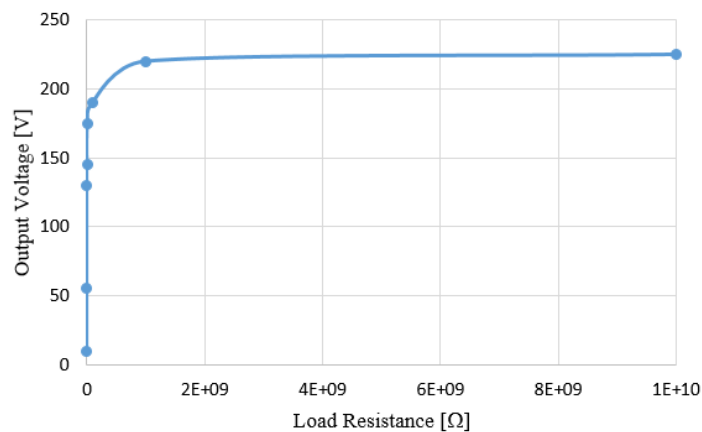


**Figure 10.**Output voltage versus load resistance.

## 5. Conclusions

A bistable piezoelectric energy harvester was comprehensively simulated in this paper. First, two previous studies were linked together in order to obtain the equivalent values for stiffness, electromechanical coupling and capacitance coefficients of the piezoelectric cantilever beam. Second, numerical models were developed to simulate the electromechanical, electrostatic, magnetic repulsion force, Eigen-frequency analysis and dynamic time responses for the proposed harvester. In order to examine each numerical module used in this work, a commercial unimorph piezoelectric cantilever beam and nickel-plated NdFeB couple of magnets have been selected. Moreover, a comparative analysis has been discussed to compare finite elements results with other values from previous research or commercial datasheet for piezoelectric beam and repelling magnets. Comparing data shows good convergence between numerical models results and previous studies. Finally, depending on finite element models results, electromechanical ordinary differential equations of the proposed bistable piezoelectric harvester have been numerically solved at a wide range of load resistance.

## References

- [1] Abdelnaby M A and Arafa M 2016 *J. Intell. Mater. Syst. Struct.* **27**(19).
- [2] Liu H, Zhang S, Kathiresan R, Kobayashi T and Lee C 2012 *Appl. Phys. Lett.* **100**(22) pp 2012-2015.
- [3] Dinulovic D, Brooks M, Haug M and Petrovic T 2015 *Phys. Procedia* **75** pp 1244–1251.
- [4] Leland E S and Wright P K 2006 *Smart Mater. Struct.* **15**(5) pp 1413–1420.

- [5] Masana R and Daqaq M F 2011 *J. Vib. Acoust. Trans. ASME* **133**(1).
- [6] Sazonov E, Pillay P, Li H, and Curry D 2009 *IEEE Sens. J.* **9** (11) pp 1422–1429.
- [7] Rhimi M and Lajnef N 2012 *J. Intell. Mater. Syst. Struct.* **23**(15) pp 1759–1770.
- [8] Chew Z J, Ruan T and Zhu M 2016 *Procedia Eng.* **168** pp 1717–1720.
- [9] Bonessio N, Zappi P, Benzoni G, Rosing T S, and Lomiento G 2016 *Open Constr. Build. Technol. J.* **10** (1) pp 136–149.
- [10] Cao S and Li J 2017 *Adv. Mech. Eng.* **9**(4) pp 1–14.
- [11] Harne R L, Thota M, and Wang K W 2013 *Smart Mater. Struct.* **22**(12).
- [12] Harne R L and Wang K W, 2013 *Smart Mater. Struct.* **22** (2).
- [13] Pellegrini S P, Tolou N, Schenk M, and Herder J L 2013 *J. Intell. Mater. Syst. Struct.* **24**(11) pp 1303–1312.
- [14] Andò B, Baglio S, Maiorca F, Trigona C 2012 *Procedia Eng.* **47**(0) pp 1061–1064.
- [15] Abdelnaby M A and Arafa M 2016 *Active and Passive Smart Structures and Integrated Systems Proc. of SPIE* **9799**, **97990M**.
- [16] Stanton S C, McGehee C C, and Mann B P 2010 *Phys. D Nonlinear Phenom.* **239** (10) 640–653.
- [17] Zhu D and Beeby S P 2013 *J. Phys. Conf. Ser.* **476**(1).
- [18] Singh K A, Kumar R, and Weber R J 2015 *IEEE Trans. Power Electron.* **30**(12) pp 6763–6774.
- [19] Harris P, Arafa M, Litak G, Bowen C R, and Iwaniec J 2017 *Eur. Phys. J. B* **90**(1).
- [20] Zhou S, Cao J, Erturk A, and Lin J 2013 *Appl. Phys. Lett.* **102**(17) pp 3–6.
- [21] Stanton S C, McGehee C C, and Mann B P 2009 *Appl. Phys. Lett.* **95**(17).
- [22] Upadrashta D and Yang Y 2016 *journal of applied physic* **120** 054504-1–054504-9.
- [23] Erturk A and Inman D J 2011 *J. Sound Vib.* **330** (10) pp 2339–2353.
- [24] Park J K and Moon W K 2005 *Sensors Actuators, A Phys.* **117**(1) pp 159–167.
- [25] Peng S, Zheng X and Peng Ke 2012 *journal of micromechanics and microengineerin* **22**(6) DOI. 10.1088/0960-1317/22/6/065005.
- [26] <https://www.americanpiezo.com/>
- [27] <https://www.first4magnets.com/>